

# Colloidal Assembly Route for Responsive Colloidosomes with Tunable Permeability

Jin-Woong Kim,<sup>†,‡</sup> Alberto Fernández-Nieves,<sup>†,§</sup> Nily Dan,<sup>||</sup> Andrew S. Utada,<sup>†</sup> Manuel Marquez,<sup>§</sup> and David A. Weitz<sup>\*,†</sup>

*Harvard School of Engineering and Applied Sciences and Department of Physics, Harvard University, Cambridge, Massachusetts 02138, Amore-Pacific Co. R&D Center, 314-1, Bora-dong, Giheung-gu, Yongin-si, Gyeonggi-Do, 446-729, Korea, Interdisciplinary Network of Emerging Science and Technology (INEST) Group, Research Center, Phillip Morris USA, Richmond, Virginia 23298, and Department of Chemical and Biological Engineering, Drexel University, Philadelphia, Pennsylvania 19104*

Received July 3, 2007; Revised Manuscript Received July 23, 2007

## ABSTRACT

We present a robust and straightforward approach for fabricating a novel colloidosome system where colloidal particles are assembled to form colloidal shells on the surface of stimuli-responsive microgel scaffolds. We demonstrate that the structural properties of the colloidal shells can be controlled through the colloidal particle size and modulus, and the state of supporting microgel particles. This technique offers a new way to engineer colloidosomes, enabling fine control over their permeability over a wide range of length scales.

Colloidosomes are hollow capsules whose shell is composed of closely packed uniform colloidal particles.<sup>1–4</sup> Like their liposome or polymersome counterparts, colloidosomes can encapsulate materials whose release rate is set by the properties of the shell. The inherent rigidity of the colloidosome shell offers mechanical advantages by comparison to the soft, self-assembled shell of liposomes or polymersomes. Moreover, the permeability of colloidosomes for encapsulated species, which is critically dependent on the size of the interstitial pores between the particles in the shell, can be tailored through variation of the dimensions of the colloidal particles.<sup>1,5–9</sup> The ability to vary the pore size of the colloidosomes makes them suitable for a wide variety of applications in pharmaceuticals, food technology, and the cosmetics industry.

To date, colloidosomes have been fabricated using colloidal assembly at liquid–liquid interfaces.<sup>10–15</sup> The resulting capsules have a high permeability to macromolecules and nanoscale species due to the large interstitial voids typically

obtained with packings of colloidal particles.<sup>12,16,17</sup> Moreover, the release of larger encapsulated materials from such traditional colloidosomes relies on external triggers such as changes in osmotic pressure or mechanical forces to crush or break open the capsule; this precludes precise control of the release response. These limitations highlight the need for a flexible technique to fabricate colloidosomes that enables both control of the permeability to small species and a high degree of sensitivity to a release trigger.

In this letter, we introduce a novel fabrication method for colloidosomes where colloidal particles with different sizes, ranging from nanometers to micrometers, are uniformly assembled to form colloidal shells on the surface of a temperature-sensitive microgel scaffold. Our approach entails a water-based rather than oil-based emulsion system. We utilize the electrostatic interactions between monodisperse charged colloidal particles and scaffolds made of microgel.<sup>18,19</sup> These electrostatic interactions dominate over thermal fluctuations, resulting in the formation of uniform shells even with nanoscale particles. The structures and permeability of the colloidal shell can be controlled by exploiting the temperature response of the microgel scaffold, which undergoes a phase transition and shrinks at higher temperatures. This provides a robust method to engineer a novel responsive colloidosome whose permeability can be finely tuned over a wide range of length scales of different encapsulated species.

\* Corresponding author. E-mail: weitz@seas.harvard.edu. Telephone: 617-496-2842. Fax: 617-495-2875. Address: Harvard School of Engineering and Applied Sciences and Department of Physics, Harvard University, Pierce Hall 231, 29 Oxford Street, Cambridge, Massachusetts 02138.

<sup>†</sup> Harvard School of Engineering and Applied Sciences and Department of Physics, Harvard University.

<sup>‡</sup> Amore-Pacific Co. R&D Center.

<sup>§</sup> Interdisciplinary Network of Emerging Science and Technology (INEST) Group, Research Center.

<sup>||</sup> Department of Chemical and Biological Engineering, Drexel University.

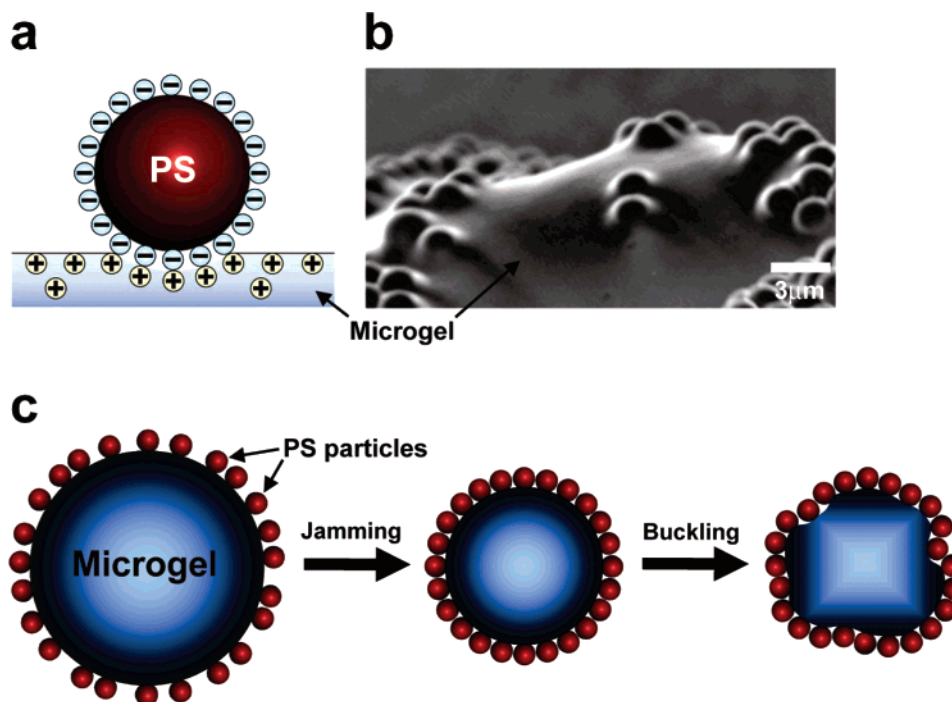


**Figure 1.** Fabrication of responsive colloidosomes. (a) Schematic for the electrostatic attraction between the positively charged microgel and negatively charged PS particles. (b) A scanning electron microscope (SEM) micrograph of the PS particles (2  $\mu\text{m}$ , sulfate-functionalized, Invitrogen) that are partially embedded in the surface of a microgel. (c) Schematic showing the jamming and buckling processes of monodisperse colloid particles on the surface of microgels. The surface area of the microgels is controlled by changing the temperature.

We generate monodisperse temperature-responsive microgel particles using microfluidics (see Supporting Information).<sup>20,21</sup> We synthesize poly(*N*-isopropylacrylamide) (PNIPAm)-based microgels that are crosslinked with  $\sim 7.5\%$  w/v *N,N'*-methylenebisacrylamide and copolymerized with  $\sim 20\%$  [2-(methacryloyloxy) ethyl trimethyl ammonium chloride], which gives rise to positive charges in the gel network. The diameters of microgel particles used in this study are approximately 50, 120, and 620  $\mu\text{m}$ . To fabricate the colloidosomes, we use negatively charged polystyrene (PS) particles ranging in diameter from 20 nm to 4  $\mu\text{m}$  and mix in excess concentration with the microgels; they adsorb the microgel scaffold due to electrostatic interactions, as illustrated in Figure 1a,b. Initially, the PS particles only partially cover the microgel surface (Figure S1, Supporting Information). However, increasing the temperature to reduce the volume of the microgel decreases the average distance between adsorbed colloidal particles, thereby leading to more complete surface coverage (Figure 1c and Supporting Information Movie S1).

As the surface area of the microgel particles is reduced, the adsorbed particles form a single packed layer with some crystalline order, as shown in Figure 2a. Further decreasing the surface area of the microgel by increasing the temperature causes the particles to jam in an amorphous state that may buckle, as shown in an electron microscope image of Figure 2b. This results in a multilayered buckled shell, where the particles are linked through the microgel, thereby creating a dense yet porous coating, as can be seen in the inset of Figure 2b. The small linkages between the particles in this image are the microgel. The degree of buckling typically depends on the degree to which the microgel shrinks after

the particles jam; this also ultimately determines the thickness of the buckled colloidal layer.

Although buckling always occurs after jamming, the topology of the buckled layers varies with the size of the PS particles for a given microgel size: PS particles with sizes of micrometers buckle to form bumpy colloidal shells (Figure 2b), whereas PS particles less than 500 nm exhibit a multifolded wrinkled topology upon buckling (Figure 3a,b). We also have measured the thickness of the buckled layers by fracturing dried colloidosomes, as shown in Figure 3c. Unlike the thickness of single-layered colloidal shells, which scales linearly with particle size, the thickness of the buckled layers is insensitive to the size of the adsorbed particle. This indicates that the buckling process is determined solely by the decrease in surface area of the microgel particles as they shrink irrespective of the colloidal particle size.

The collapse temperature of the colloidosomes decreases with decreasing colloid particle size, as shown in Figure 3d: 500 nm PS particles do not affect the transition temperature, while 80 nm PS particles reduce it by  $\sim 10^\circ\text{C}$  and 20 nm PS particles reduce it by  $\sim 30^\circ\text{C}$ . This effect is independent of the type of ionic group responsible for the particle charge, as identical behavior is observed with 20 nm sulfated PS particles and 20 nm carboxylated PS particles. The dependence of the transition temperature on colloid particle size suggests that the transition is controlled predominantly by the charge near the surface of the microgels because the total charge neutralization due to the particle adsorption increases as the colloid particle size decreases (Supporting Information). The importance of the surface charge in determining the transition temperature implies that the charge is not homogeneously distributed in the microgel but is instead

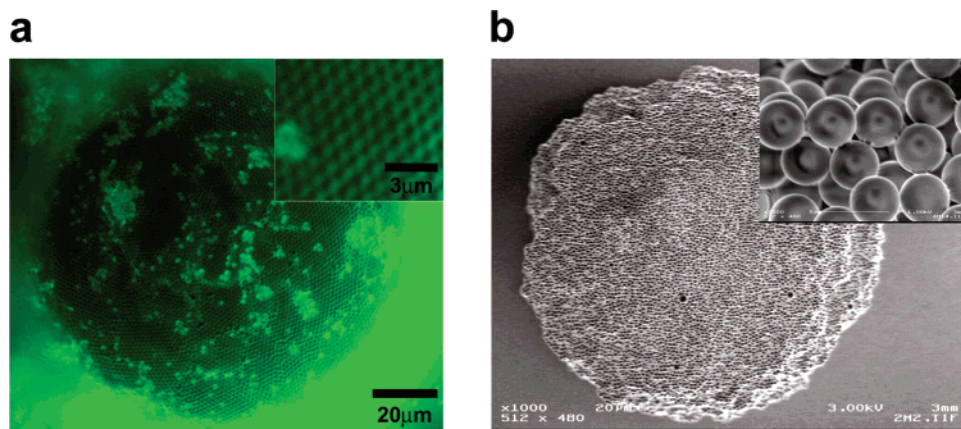


**Figure 2.** Microgels covered with colloidal particles. (a) Fluorescence microscope image of jammed PS particles on the surface of a microgel. Using fluorescein-labeled PS particles ( $1\ \mu\text{m}$ , sulfate-functionalized) to make colloidosomes allows us to image the jammed particles. Inset: high-magnification image of the jammed PS particles showing the nearly crystalline order. Jamming of the PS particles occurs at  $\sim 50\ ^\circ\text{C}$ . (b) SEM micrograph of the buckled surface of a colloidosome consisting of PS particles ( $1\ \mu\text{m}$ , sulfate-functionalized). Inset: high-magnification image of the colloid shell ( $4\ \mu\text{m}$ , sulfate-functionalized PS particles). Close inspection reveals the presence of the microgel linking the particles together. The buckled layers were observed after completely drying colloidosomes at  $60\ ^\circ\text{C}$  for 24 h.

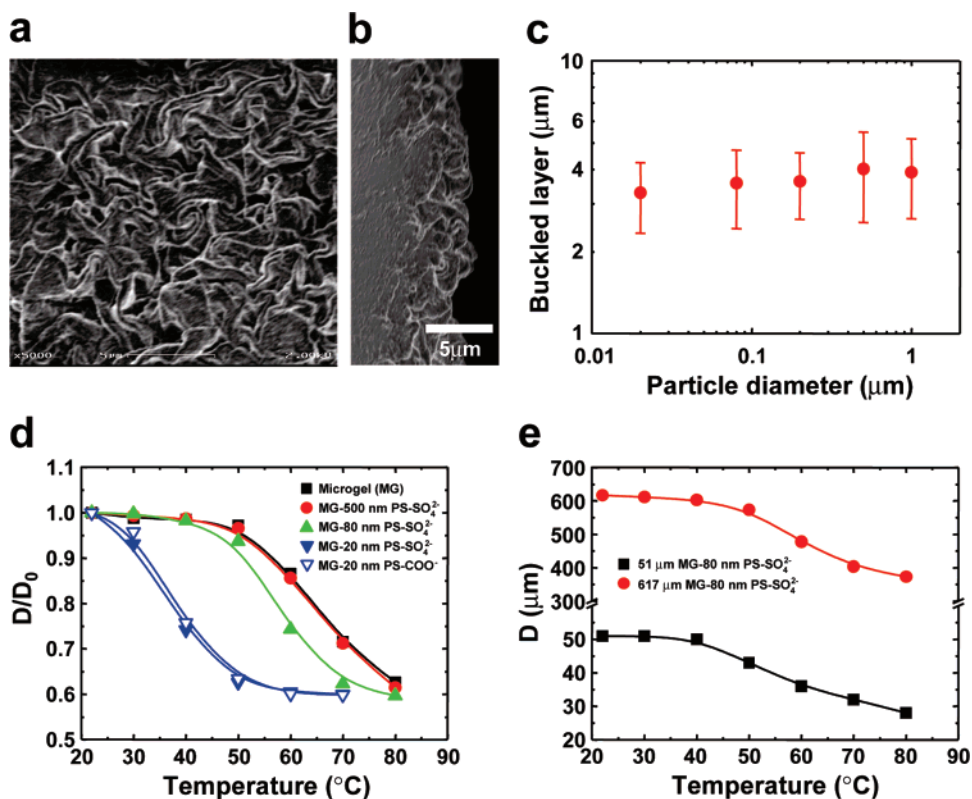


**Figure 3.** Phase properties of responsive colloidosomes. (a) SEM micrograph of a buckled surface consisting of nanosized PS particles (80 nm, sulfate-functionalized). (b) SEM micrograph of a fractured layer. This sample is the same as that in Figure 3a. (c) Thickness of buckled layers as a function of the size of the PS particles (sulfate-functionalized). (d) Phase transitions of colloidosomes with different diameters of PS particles (sulfate-functionalized). To confirm the effect of the type of ions, we also prepared colloidosomes with carboxylate-functionalized PS particles (20 nm) and measured their phase transitions. (e) Phase transitions of colloidosomes with different diameters of microgel particles; 51 and 617  $\mu\text{m}$ . In this case, we made colloidosomes with 80 nm PS particles. Here we measured the change of the diameter of colloidosomes,  $D$ , normalized by the initial diameter,  $D_0$ , vs temperature,  $T$ .

more concentrated at the periphery;<sup>22,23</sup> this may reflect the effect of the rapid reaction rate of the crosslinker, which is faster than all the components, causing an increased concentration in the center of the microgel, which prevents charge dissociation, thereby reducing the charge in the center relative to that at the periphery. Further support for this

comes from comparison of the transition temperature for colloidosomes made from different size of microgels but the same size PS particles. The transition temperature is identical for all cases, as shown in Figure 3e, confirming that the gel collapse is dominated by surface rather than bulk charges and it is significantly affected by small PS particles.



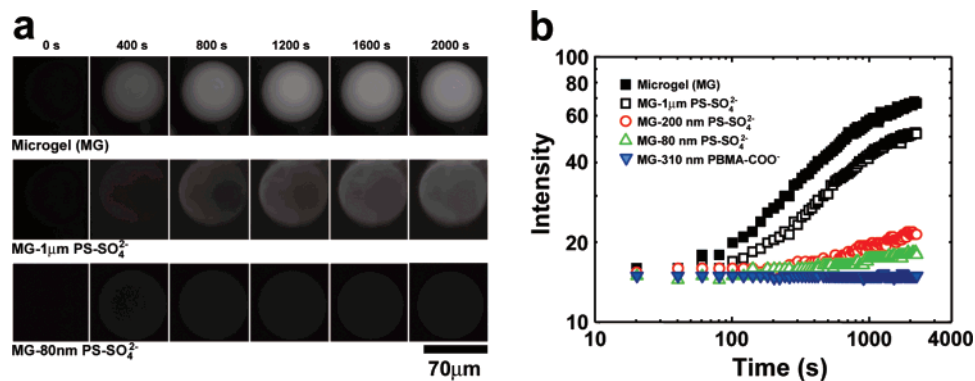


**Figure 4.** Permeability of responsive colloidosomes. (a) Time series of fluorescence images showing the permeation of fluorescein sodium salts into a plain microgel (upper) and colloidosomes made with 1  $\mu\text{m}$  PS particles (middle) and 80 nm PS particles (lower). Time begins after the first detection of fluorescence. The flow of a dilute aqueous fluorescein sodium salt solution (0.5  $\mu\text{M}$ ) in a square glass capillary tube (1 mm inner dimension) was set at 500  $\mu\text{L}\cdot\text{h}^{-1}$ , using a syringe pump (Harvard Apparatus). Experiments were conducted at 65  $^{\circ}\text{C}$ , set by a temperature-controlled stage on a fluorescence microscope (Leica). (b) Effect of particle diameter and deformability on the permeability of fluorescein molecules through the colloid shells. The fluorescence intensity measurements for all the PS particles were conducted at 65  $^{\circ}\text{C}$ . We also measured the fluorescence intensity for colloidosomes covered with poly(butyl methacrylate) (PBMA) particles (310 nm, carboxylate-functionalized) at 25  $^{\circ}\text{C}$ . PBMA particles were synthesized by using the emulsion polymerization technique (see Supporting Information).

The permeability of colloidosomes can be controlled through the size of the colloidal particles.<sup>1,5–9</sup> To test the relationship between particle diameter and permeability, we measure the fluorescence intensity inside the colloidosomes as a function of time while they are immersed in a flowing aqueous solution containing fluorescein molecules; here we exploit the positive charge of the gel network to actively draw in the negatively charged fluorescein ions. In colloidosomes that do not undergo the buckling transition, we observe that fluorescein molecules readily pass through the colloid shells. By contrast, in the buckled state, the permeability decreases significantly with decreasing colloidal particle size, as shown in Figure 4; for the 80 nm PS particles, the penetration of fluorescence molecules is largely suppressed, indicating that the dense, complex colloidal layers block transport of the fluorescein molecules. As expected, cooling buckled colloidosomes causes them to expand, leading to nonuniform coverage of the microgel surface by the colloidal particles, thereby again increasing the permeability.

The colloidosome permeability can be tailored by changing the dimension of the adsorbed colloidal particles, the overall shell thickness, and the degree of fusion between the colloidal particles. In systems composed of solid particles, heat can be used to induce fusion. Alternatively, fusion can be induced through the use of particles that deform under stress. To explore this possibility, we use negatively charged poly(butyl methacrylate) (PBMA) particles that have a glass transition temperature,  $T_g$ , of approximately 30  $^{\circ}\text{C}$ .<sup>24,25</sup> The average diameter of the PBMA particles is 310 nm, so that if they were rigid, we would expect the permeability to be higher than that of the 200 nm PS particles (see Figure 4). However, the PBMA particles can pack more closely on the gel surface, even at room temperature, due to their deformability close to their  $T_g$ . As a result, fluorescence permeation is inhibited more effectively with this colloidal shell, not only by comparison with rigid PS particles of comparable size, but also by comparison to shells composed of much smaller

particles (80 nm), as shown in Figure 4. In fact, with deformable particles, the permeability can be inhibited even without inducing buckling.

In conclusion, we present a robust means of fabricating responsive colloidosomes by covering the surface of temperature-sensitive microgels with colloidal particles that can range in size from nanometers to micrometers. This technique enables control of the permeability of the colloidosome shell in several ways: through the size of the adsorbed colloidal particles, the thickness of the particle shell, obtained by buckling the microgel surface, or through the use of deformable particles. The advantage of using a temperature-responsive microgel as a colloidosome scaffold is the ability not only to tailor the shell thickness but also to manipulate the permeability through changes in the temperature. Using scaffolds of other stimuli-responsive polymers will enable the design of controlled release colloidosome capsules whose permeability responds to different triggers.

**Acknowledgment.** This work was supported by the Postdoctoral Fellowship Program of Korea Research Foundation (KRF) and by the NSF (DMR-0602684) and the Harvard MRSEC (DMR-0213805). A.F.-N. is grateful to Junta de Andalucía and to University of Almería (leave of absence).

**Supporting Information Available:** Detailed experimental methods. Uniform colloidosomes covered with colloidal particles (Figure S1). A bright field microscope image of a colloidosome after a heating and cooling cycle (Figure S2). A movie for the phase transition of a colloidosome (Movie S1). Model derivation for responsive colloidosomes (Figures S3 and S4) (ZIP). This material is available free of charge via the Internet at <http://pubs.acs.org>.

## References

- (1) Dinsmore, A. D.; Hsu, M. F.; Nikolaides, M. G.; Marquez, M.; Bausch, A. R.; Weitz, D. A. *Science* **2002**, 298, 1006–1009.

- (2) Gordon, V. D.; Chen, X.; Hutchinson, J. W.; Bausch, A. R.; Marquez, M.; Weitz, D. A. *J. Am. Chem. Soc.* **2004**, *126*, 14117–14122.
- (3) Velev, O. D.; Furusawa, K.; Nagayama, K. *Langmuir* **1996**, *12*, 2374–2384.
- (4) Velev, O. D.; Nagayama, K. *Langmuir* **1997**, *13*, 1856–1859.
- (5) Duan, H. W.; Wang, D. Y.; Sobal, N. S.; Giersig, M.; Kurth, D. G.; Möhwald, H. *Nano Lett.* **2005**, *5*, 949–952.
- (6) Reincke, F.; Hickey, S. G.; Kegel, W. K.; Vanmaekelbergh, D. *Angew. Chem., Int. Ed.* **2004**, *43*, 458–462.
- (7) Binks, B. P.; Murakami, R.; Armes, S. P.; Fujii, S. *Angew. Chem., Int. Ed.* **2005**, *44*, 4795–4798.
- (8) Cayre, O. J.; Noble, P. F.; Paunov, V. N. *J. Mater. Chem.* **2004**, *14*, 3351–3355.
- (9) Noble, P. F.; Cayre, O. J.; Alargova, R. G.; Velev, O. D.; Paunov, V. N. *J. Am. Chem. Soc.* **2004**, *126*, 8092–8093.
- (10) Binks, B. P. *Curr. Opin. Colloid Interface Sci.* **2002**, *7*, 21–41.
- (11) Binks, B. P.; Clint, J. H. *Langmuir* **2002**, *18*, 1270–1273.
- (12) Lin, Y.; Skaff, H.; Emrick, T.; Dinsmore, A. D.; Russell, T. P. *Science* **2003**, *299*, 226–229.
- (13) Pieranski, P. *Phys. Rev. Lett.* **1980**, *45*, 569–572.
- (14) Melle, S.; Lask, M.; Fuller, G. G. *Langmuir* **2005**, *21*, 2158–2162.
- (15) Lawrence, D. B.; Cai, T.; Hu, Z.; Marquez, M.; Dinsmore, A. D. *Langmuir* **2007**, *23*, 395–398.
- (16) Duan, H. W.; Wang, D. Y.; Kurth, D. G.; Möhwald, H. *Angew. Chem., Int. Ed.* **2004**, *43*, 5639–5642.
- (17) Lin, Y.; Skaff, H.; Böker, A.; Dinsmore, A. D.; Emrick, T.; Russell, T. P. *J. Am. Chem. Soc.* **2003**, *125*, 12690–12691.
- (18) Larson, R. G. *The Structure and Rheology of Complex Fluids*; Oxford University Press: New York, 1998.
- (19) Ohshima, H. *Adv. Colloid Interf. Sci.* **1994**, *53*, 77–102.
- (20) Kim, J. W.; Utada, A. S.; Fernández-Nieves, A.; Hu, Z.; D. A. Weitz, *Angew. Chem., Int. Ed.* **2007**, *46*, 1819–1822.
- (21) Utada, A. S.; Lorenceau, E.; Link, D. R.; Kaplan, P. D.; Stone, H. A.; Weitz, D. A. *Science* **2005**, *308*, 537–541.
- (22) Parsegian, V. A.; Gingel, D. *Biophys. J.* **1972**, *12*, 1192–1204.
- (23) Ostroha, J.; Pong, M.; Lowman, A.; Dan, N. *Biomaterials* **2004**, *25*, 4345–4353.
- (24) Brandrup, J.; Immergut, E. H.; Grulke, E. A. *Polymer Handbook*, 4th ed.; John Wiley & Sons: New York, 1999.
- (25) Sugiyama, Y.; Larsen, R. J.; Kim, J. W.; Weitz, D. A. *Langmuir* **2006**, *22*, 6024–6030.

NL0715948